# Repolarization alternans in human ventricular hyperkalaemic tissue: dependence on current stimulation

V. Monasterio[1,3], J. Carro[1,3], E. Pueyo[2,3]

[1] Escuela Politécnica Superior, Universidad San Jorge, Villanueva de Gállego, España, {vmonasterio, jcarro}@usj.es

[2] CIBER-BBN, Universidad de Zaragoza, Zaragoza, España, epueyo@unizar.es

[3] BSICoS Group. Aragon Institute for Engineering Research (I3A). IIS Aragón, Zaragoza, España

## Abstract

*Computational modeling and simulation is a powerful tool to study cardiac electrical activity and investigate conditions leading to arrhythmias. Electrophysiological models of human ventricular myocytes and tissues provide detailed descriptions of action potentials (APs) in health and disease. However, simulation results heavily depend on specific parameter setups. A key parameter in cardiac simulations is the stimulus current ($I_{stim}$), whose value is commonly set based on the determined diastolic threshold. The use of empirical* ad hoc *rules to find the diastolic threshold may strongly impact simulation results. In this study we compared three ways of determining the diastolic threshold in 1-D tissue simulations for the study of AP alternans. Three different definitions of 'successful propagation' were considered in order to find the diastolic threshold: the first one was based on the amplitude of a single AP, the second one was based on the amplitude of five consecutive APs, and the third one was based on the AP duration (APD) of five consecutive APs. According to our results, the most appropriate definition of 'successful propagation' was the third one. In that case, simulations of severe hyperkalemia showed AP alternans and changes in AP shape that are consistent with observations from* in silico *and* in vivo *experiments during acute ischemia.*

## 1. Introduction

Repolarization alternans (RA) is a phenomenon that appears in the electrocardiogram (ECG) as a consistent fluctuation in the morphology of the ventricular repolarization on an every-other-beat basis. RA reflects spatio-temporal heterogeneity of repolarization, and arises from beat-to-beat alternation of action potential (AP) duration (APD) at the level of cardiac myocytes [1][2].

RA has been associated with an increased risk for malignant ventricular arrhythmias and sudden cardiac death across a wide range of pathophysiological conditions, including ischemic heart disease [1][2]. The mechanisms underlying RA and its link to vulnerability are still not completely known, and may be different depending on the accompanying clinical conditions. During acute ischemia, the main physiological changes that occur in cardiomyocytes are hypoxia, acidosis, and hyperkalaemia (that is, an increase in the extracellular potassium concentration $[K^+]_o$) [3]. The exact role of these factors in the genesis of alternans leading to arrhythmic events is not fully understood yet.

In recent years, computational simulation has become a powerful tool that complements experimental and clinical research when studying arrhythmic mechanisms. Electrophysiological models of human ventricular myocytes are able to simulate transmembrane ionic currents and APs with a great degree of electrophysiological detail [4]. Tissue models built on them provide qualitative and quantitative descriptions of AP propagation. Results from such models, however, are strongly dependent on simulation setups. For example, a basic step in cardiac simulations is the application of a stimulus current ($I_{stim}$) in order to trigger the AP response. The value of $I_{stim}$ is usually set to 1.5 to 2 times the diastolic threshold, which is defined as the minimum current that produces a successful propagation of the electrical impulse. In practice, the diastolic threshold is determined empirically using *ad hoc* rules to decide whether propagation is successful or not [5][6][7]. Such rules may vary from one study to another, and may have a strong influence on the simulated results.

In this work, we use a recent human ventricular AP model (the CRLP model [5]) to explore three alternative ways of determining the diastolic threshold in 1-D tissue simulations. We compare the results with those obtained in single cells and analyze the implications of each of the three definitions for the study of cardiac alternans under hyperkalaemic conditions.

## 2. Methods

Simulations were carried out using the software ELVIRA [4][8], following the approach described in Carro et al. [5]. Hyperkalaemic conditions were simulated by increasing $[K^+]_o$ from 4 to 10 mM with 0.1-mM steps.

### 2.1. Single-cell simulations

For single-cell simulations, the system of differential equations that govern the cellular electrical behavior according to the epicardial CRLP model [5] was solved by using forward Euler integration with a time step $\Delta t$ = 0.002 ms. The transmembrane potential ($V_m$) and all the other state variables were computed at each time step.

For each $[K^+]_o$ value, we determined the diastolic threshold ($I_{threshold}$) in three alternative ways, as described below. In all cases, the model was first allowed to reach steady-state, as in [5]. Then, the cell was stimulated with a train of 5 current pulses of 1-ms duration delivered at a cycle length (CL) of 1000 ms. We varied the stimulus current amplitude in 0.1 pA/pF steps until we found the

minimum amplitude, $I_{threshold}$, that produced either (a) a single AP with maximum $V_m \geq 0$ mV (*single AP definition*) or (b) five APs with maximum $V_m \geq 0$ mV (*multiple APs definition*) or (c) five consecutive APs with $APD_{90}$ (APD at 90% repolarization) ≥ 150 ms (*APD-based definition*). The limit of 150 ms was chosen empirically, after visual inspection of successfully- and unsuccessfully-triggered APs in the simulations.

After determining the diastolic threshold with each of the alternatives (a), (b) and (c), the cell was stabilized again and was finally stimulated with a train of 10 pulses with an amplitude of twice $I_{threshold}$ and 1-ms duration, at a CL of 1000 ms (*S1 protocol*).

### 2.2. 1-D tissue simulations

For tissue simulations, we created a homogeneous 4-cm long fiber composed of epicardial cells. Electric propagation across the cardiac tissue was modeled with a monodomain reaction-diffusion equation. Discretization was performed using a space step of $\Delta x = 0.1$ mm and a time step of $\Delta t = 0.002$ ms. A value of $\sigma = 0.0013$ $cm^2$ $ms^{-1}$ for the diffusion coefficient was used. The system of equations was solved using the conjugate gradient method. Five positions within the fiber were selected for further analysis in each simulation; those positions were located at 1.5, 1.75, 2, 2.25 and 2.5 cm from the stimulation end of the cable.

For each $[K^+]_o$ value, we determined the diastolic threshold in three alternative ways. In all cases the model was stabilized as described in Section 2.1. Then, one end of the fiber was stimulated with a train of 5 current pulses of 1-ms duration. We repeated these two operations with different current amplitudes, in 0.1 pA/pF steps, until we found the minimum amplitude, $I_{threshold}$, that produced successful propagation along the fiber as defined next. Three alternative definitions of 'successful propagation' were explored: (a) a single AP propagates along the fiber with maximum $V_m \geq 0$ mV (*single AP definition*); (b) five consecutive APs propagate along the fiber with maximum $V_m \geq 0$ mV (*multiple APs definition*); and (c) five consecutive APs propagated along the fiber with duration $APD_{90} \geq 150$ ms (*APD-based definition*). In all cases, an upper limit of 1000 pA/pF was set for the search of $I_{threshold}$, since such value was one order of magnitude higher than the rest of currents in the model.

After determining the diastolic threshold with alternatives (a), (b) and (c), the model was stabilized again, and then the fiber was stimulated with a train of 10 pulses with an amplitude of twice $I_{threshold}$ and 1-ms duration, delivered at a CL of 1000 ms (*S1 protocol*).

## 3. Results

### 3.1. Single-cell simulations

The diastolic threshold computed with the *single AP* definition decreased from 24.6 pA/pF to 13.7 pA/pF for increasing $[K^+]_o$ (Figure 1). The diastolic thresholds computed with the *multiple APs* and the *APD-based* definitions yielded very similar results to those of the *single AP* definition for every tested $[K^+]_o$, decreasing from 24.6 pA/pF to 14.4 pA/pF for increasingly higher $[K^+]_o$ (Figure 1).

No AP alternans was observed for any $[K^+]_o$ value following stimulation with the described S1 protocol in any case.

### 3.2. 1-D tissue simulations

When the *single AP* definition was considered, the diastolic threshold decreased monotonically from 255 pA/pF to 130 pA/pF for increasing $[K^+]_o$ (Figure 2). At $[K^+]_o$ = 10 mM, alternation between complete and incomplete APs appeared during S1 stimulation in all computed positions along the fiber (Figure 3).

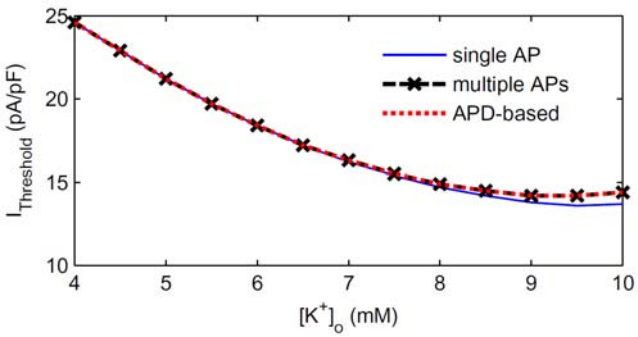


***Figure 1.*** *Diastolic threshold for single-cell simulations*

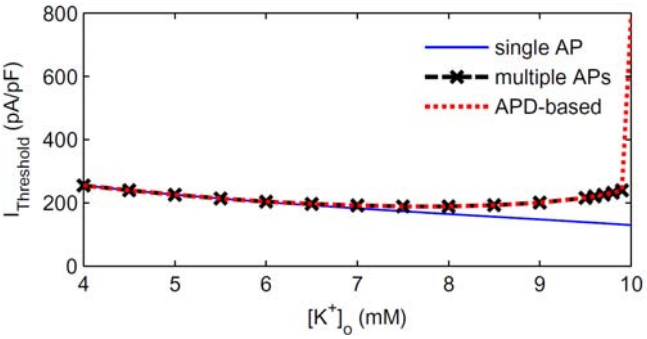


***Figure 2.*** *Diastolic threshold for fiber simulations*

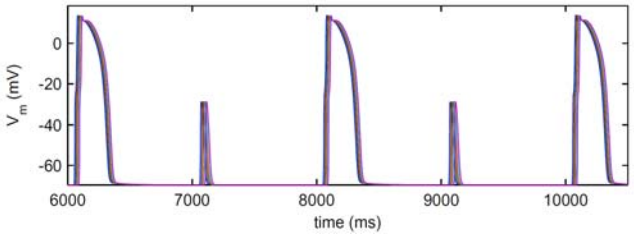


***Figure 3.*** *S1 protocol for $[K^+]_o$ =10 mM. The fiber was stimulated at twice the diastolic threshold as determined with the single AP definition ($I_{stim}$ = 260 pA/pF). Each color represents a different position in the fiber (blue: 1.5 cm, green: 1.75 cm, red: 2 cm, cyan: 2.25, and magenta: 2.5 cm).*

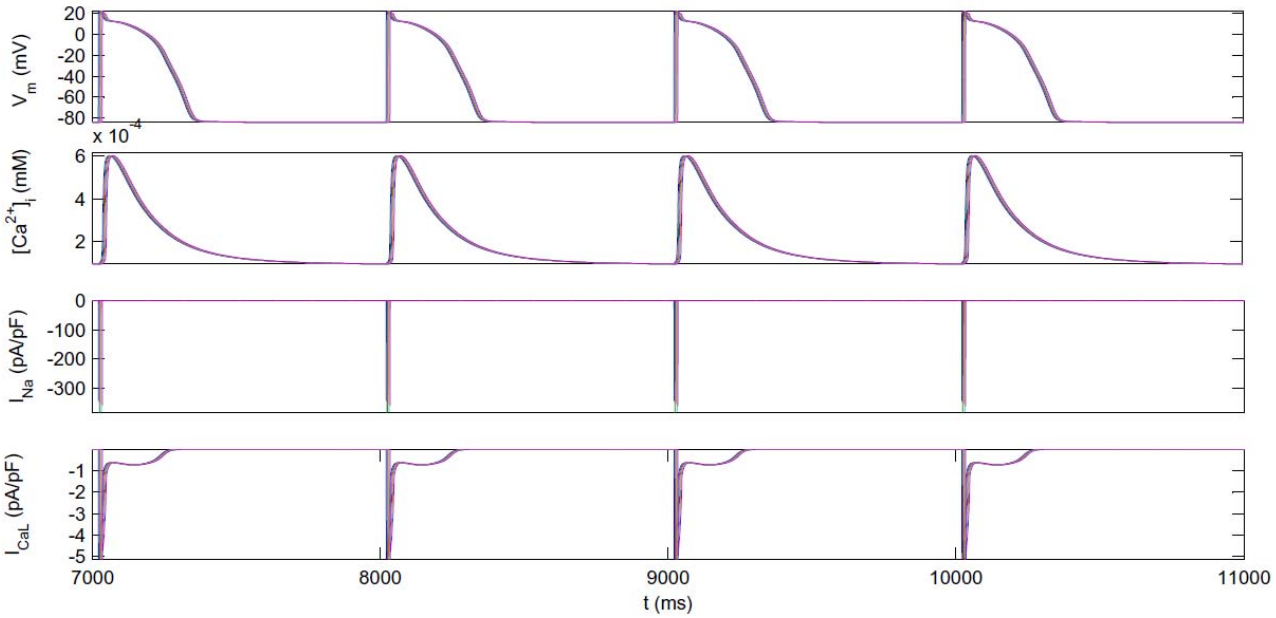


***Figure 4.*** *S1 protocol for $[K^+]_o$ =5.4 mM (control conditions). Stimulation at twice the diastolic threshold as determined with the APD-based definition ($I_{stim}$ = 1578 pA/pF). Each color represents a different position in the fiber.*

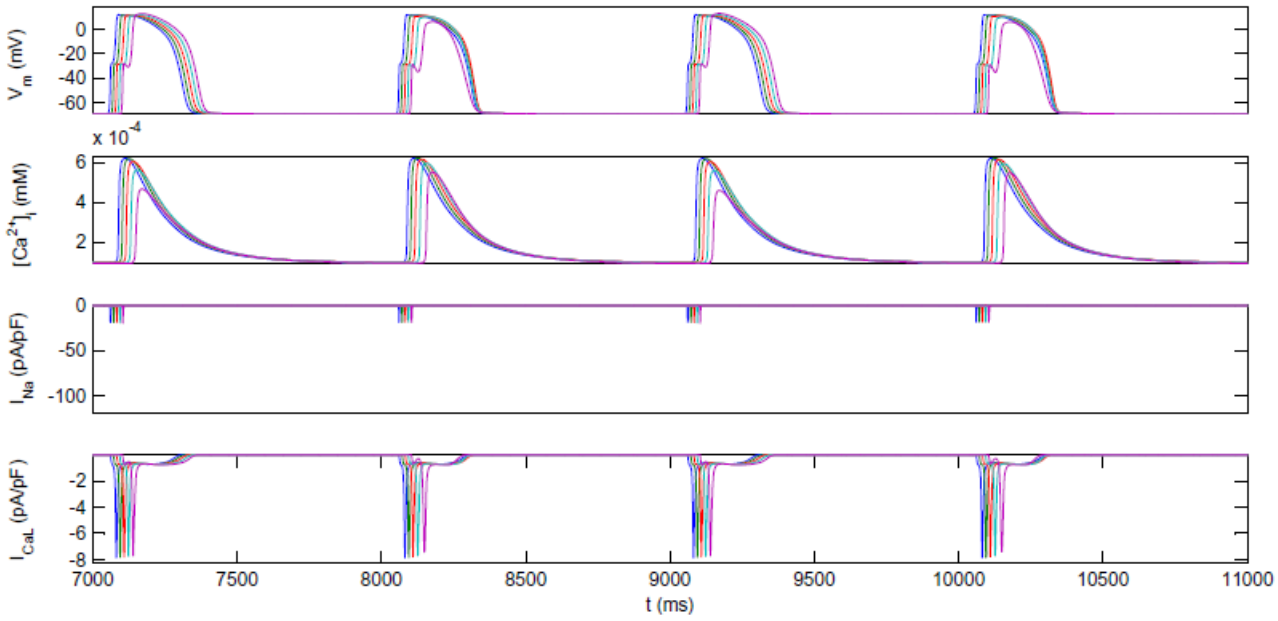


***Figure 5.*** *S1 protocol for $[K^+]_o$ =10 mM. Stimulation at twice the diastolic threshold as determined with the APD-based criterion ($I_{stim}$ = 1578 pA/pF). Each color represents a different position in the fiber (blue: 1.5 cm, green: 1.75 cm, red: 2 cm, cyan: 2.25, and magenta: 2.5 cm)*

When the *multiple APs* definition was considered, the diastolic threshold decreased from 255 pA/pF ($[K^+]_o$ = 4 mM) to 189 pA/pF ($[K^+]_o$ = 7.5 mM), and then increased again up to 240 pA/pF for $[K^+]_o$ = 9.9 mM (Figure 2). For $[K^+]_o$ = 10 mM there was no propagation, even with the limit of $I_{threshold}$ = 1000 pA/pF. No AP alternans was observed for any $[K^+]_o$ during S1 stimulation.

When the *APD-based* definition was considered, the diastolic threshold decreased from 255 pA/pF ($[K^+]_o$ = 4 mM) to 189 pA/pF ($[K^+]_o$ = 7.5 mM), and then increased again up to 240 pA/pF for $[K^+]_o$ = 9.9 mM and to 789 pA/pF for $[K^+]_o$ = 10 mM (Figure 2). For $[K^+]_o \leq$ 9.9 mM, no AP alternans was observed during S1 stimulation. As an example, Figure 4 depicts results for $[K^+]_o$ = 5.4 mM, which is the default value in the CRLP model. However, for $[K^+]_o$ = 10 mM, AP alternans appeared at distal positions in the fiber during S1 stimulation (Figure 5).

Also, for $[K^+]_o \geq$ 9.9 mM the AP shape varied substantially with respect to the normal shape: The AP

upstroke was divided into two components, the first one supported by $I_{Na}$, and the second one supported by $I_{CaL}$ (Figure 5).

To evaluate whether the appearance of AP alternans and the change in AP shape were independent of the stimulation current $I_{stim}$, S1 stimulation was repeated with $I_{stim}$ = 2000 pA/pF. Both phenomena were observed again, with no substantial changes with respect to the simulations where $I_{stim}$ was set at twice the diastolic threshold.

## 4. Discussion and conclusions

In this study we compared three ways of determining the diastolic threshold in 1-D tissue simulations for the study of AP alternans. According to our results, the most appropriate definition of 'successful propagation' was the one based on the APD of five consecutive impulses.

The *single AP* definition produced spurious alternans-like patterns such as those depicted in Figure 3. AP alternans has been linked to abnormalities in intracellular Ca dynamics [1]. The coupling between APD and Ca dynamics is a complex process, and the mechanisms behind AP alternans are not completely understood yet [2]. Nevertheless, no dependency between AP alternans and stimulation current amplitude has been reported in the literature, and therefore the alternans pattern found in this case should be disregarded as a methodological artefact, since it disappeared with a high enough stimulation amplitude.

On the other hand, when the rule based on multiple APDs was considered, simulations of severe hyperkalaemia produced alternans patterns that were independent of the stimulation current amplitude. The first measured position in the fiber showed no alternation (a behavior similar to that of an isolated cell), whereas an alternating pattern appeared along the fiber as a result of both hyperkalaemia and propagation effects. Also, the change in AP shape observed during severe hyperkalaemia was found to be consistent with observations from *in silico* [7] and *in vivo* [9] experiments during acute ischemia.

Several limitations of this work need to be acknowledged. First, the present study investigates the response of human epicardial cells and tissues to hyperkalaemia, while the the effects of hypoxia and acidosis are not included and, thus, the results do not represent a response to acute ischemia, but only to hyperkalaemia. Second, we investigated changes in the stimulus current diastolic threshold after varying $[K^+]_o$, but we did not look into the mechanisms underlying the observed non-monotonic change in $I_{threshold}$ with increasingly higher $[K^+]_o$. While for mild to moderate hyperkalaemia a decrease in $I_{threshold}$ with increasing $[K^+]_o$ can be expected in correspondence with shortened APD and elevated resting potential [7], the increase in $I_{threshold}$ for severe hyperkalaemia deserves further investigation.

## Acknowledgements

This work was supported by projects TIN2013-41998-R and TEC2010-19410 by MINECO (Spain) and by BSICoS Group (T96) from Government of Aragon and European Social Fund (EU). CIBER is a center of the Instituto de Salud Carlos III with assistance from the European Regional Development Fund (FEDER). E.P. acknowledges the financial support of Ramón y Cajal program from MINECO.

## References

[1] Gaeta SA, Christini DJ. Non-linear dynamics of cardiac alternans: subcellular to tissue-level mechanisms of arrhythmia. *Frontiers in physiology*, 2012, vol 3.

[2] Weiss JN, Nivala M, Garfinkel A, Qu Z. Alternans and Arrhythmias: From Cell to Heart. *Circulation Research*, 2011, vol 108, pp 98–112.

[3] Carmeliet E. Cardiac ionic currents and acute ischemia: from channels to arrhythmias. *Physiological Reviews,* vol 79, 1999, pp 917–1017.

[4] Niederer SA, Kerfoot E, Benson AP, Bernabeu MO, Bernus O, Bradley C, et al. Verification of cardiac tissue electrophysiology simulators using an n-version benchmark. *Philosophical Transactions Royal Society A*, vol 369, 2011, pp 4331–51.

[5] Carro J, Rodríguez JF, Laguna P, and Pueyo E. A human ventricular cell model for investigation of cardiac arrhythmias under hyperkalaemic conditions, *Philosophical Transactions Royal Society A*, vol 369, 2011, pp 4205–32.

[6] Dutta, S., Mincholé, A., Quinn, T. A., and Rodriguez, B. Recent human ventricular cell action potential models under varied ischaemic conditions. In *Computing in Cardiology Conference (CinC)*, 2013. pp. 695-698.

[7] Ferrero JM, Trénor B, Rodriguez B, Saiz J. Electrical activity and re-entry during acute regional myocardial ischemia: insights from simulations. *International Journal Bifurcation and Chaos*, vol 13, 2003, 3703–15.

[8] Heidenreich E, Ferrero J, Doblare M, Rodriguez J. Adaptive macro finite elements for the numerical solution of monodomain equations in cardiac electrophysiology. *Annals of Biomedical Engineering*, vol 38, 2010, pp 2331–45.

[9] Kleber AG, Janse MJ, van Capelle FJ, Durrer D. Mechanism and time course of ST and TQ segment changes during acute regional myocardial ischemia in the pig heart determined by extracellular and intracellular recordings. *Circulation Research*, vol 42, 1978, pp 603–13.